Insight into the Electronic Structure of the CP47 Antenna Protein Complex of Photosystem II: Hole Burning and Fluorescence Study

ARTICLE *in* JOURNAL OF THE AMERICAN CHEMICAL SOCIETY · MARCH 2010

Impact Factor: 12.11 · DOI: 10.1021/ja908510w · Source: PubMed

8 AUTHORS, INCLUDING:

Nhan C Dang
Los Alamos National Laboratory
20 PUBLICATIONS **200** CITATIONS
SEE PROFILE

Mike Reppert
Massachusetts Institute of Technology
27 PUBLICATIONS **325** CITATIONS
SEE PROFILE

Ryszard Jankowiak
Kansas State University
193 PUBLICATIONS **4,702** CITATIONS
SEE PROFILE

J|A|C|S ARTICLES

Published on Web 03/10/2010

Insight into the Electronic Structure of the CP47 Antenna Protein Complex of Photosystem II: Hole Burning and Fluorescence Study†

Bhanu Neupane,‡ Nhan C. Dang,‡ Khem Acharya,‡ Mike Reppert,‡ Valter Zazubovich,§ Rafael Picorel,||,⊥ Michael Seibert,|| and Ryszard Jankowiak*,‡

Department of Chemistry, Kansas State University, Manhattan, Kansas 66506, Department of Physics, Concordia University, Montreal H4B 1R6, Quebec, Canada, and National Renewable Energy Laboratory, Golden, Colorado 80401

Received October 19, 2009; E-mail: ryszard@ksu.edu

Abstract: We report low temperature (*T*) optical spectra of the isolated CP47 antenna complex from Photosystem II (PSII) with a low-*T* fluorescence emission maximum near 695 nm and not, as previously reported, at 690−693 nm. The latter emission is suggested to result from three distinct bands: a lowest-state emission band near 695 nm (labeled F1) originating from the lowest-energy excitonic state A1 of intact complexes (located near 693 nm and characterized by very weak oscillator strength) as well as emission peaks near 691 nm (FT1) and 685 nm (FT2) originating from subpopulations of partly destabilized complexes. The observation of the F1 emission is in excellent agreement with the 695 nm emission observed in intact PSII cores and thylakoid membranes. We argue that the band near 684 nm previously observed in singlet-minus-triplet spectra originates from a subpopulation of partially destabilized complexes with lowest-energy traps located near 684 nm in absorption (referred to as AT2) giving rise to FT2 emission. It is demonstrated that varying contributions from the F1, FT1, and FT2 emission bands led to different maxima of fluorescence spectra reported in the literature. The fluorescence spectra are consistent with the zero-phonon hole action spectra obtained in absorption mode, the profiles of the nonresonantly burned holes as a function of fluence, as well as the fluorescence line-narrowed spectra obtained for the Q_y band. The lowest Q_y state in absorption band (A1) is characterized by an electron−phonon coupling with the Huang−Rhys factor *S* of ∼1 and an inhomogeneous width of ∼180 cm^{-1}. The mean phonon frequency of the A1 band is 20 cm^{-1}. In contrast to previous observations, intact isolated CP47 reveals negligible contribution from the triplet-bottleneck hole, i.e., the AT2 trap. It has been shown that Chls in intact CP47 are connected via efficient excitation energy transfer to the A1 trap near 693 nm and that the position of the fluorescence maximum depends on the burn fluence. That is, the 695 nm fluorescence maximum shifts blue with increasing fluence, in agreement with nonresonant hole burned spectra. The above findings provide important constraints and parameters for future excitonic calculations, which in turn should offer new insight into the excitonic structure and composition of low-energy absorption traps.

1. Introduction

It is well-known that oxygenic photosynthesis occurs in nature in a wide variety of very different environments. Photolytic water splitting is critical to life on our planet. The key protein complex for oxygenic photosynthesis, i.e., Photosystem II (PSII), is a membrane-bound protein assembly present in plants, algae, and cyanobacteria; this complex is able to harness visible light to split water.[1,2] The minimal protein assembly able to do this is the PSII core complex, which consists of the Mn/Ca oxygen-evolving complex (OEC),[1,3,4] two proximal antenna proteins (i.e., CP43 and CP47), and the D1/D2/Cyt b_{559} reaction center (RC), where charge separation occurs. The two core antenna complexes CP43 and CP47 are present in all oxygenic photosynthetic organisms in a constant ratio of 1:1 with respect to the RC. CP43 is more loosely bound to the D1/D2 heterodimer of the RC than is CP47, and thus, it is easier to remove from

† Abbreviations: Chlorophyll (Chl); energy (*E*); electron−phonon coupling (el-ph); excitation energy transfer (EET); excitation wavelength, λ_{ex}; fluence (f); fluorescence line-narrowing (FLN); full width at half-maximum (fwhm); hole burning (HB); Huang−Rhys factor (*S*); inhomogeneous broadening (Γ_{inh}); laser induced fluorescence (LIF); nonline narrowed (NLN); nonphotochemical hole burning (NPHB); photosynthetic complexes (PC); photochemical hole burning (PHB); phonon sideband (PSB); Photosystem I (PSI); Photosystem II (PSII); reaction center (RC); room temperature (RT); single site absorption (SSA); site distribution functions (SDF); spectral hole-burning (SHB); species-associated difference spectra (SADS); temperature (*T*); mean phonon frequency (ω_m); zero-phonon line (ZPL).

‡ Kansas State University.

§ Concordia University.

|| National Renewable Energy Laboratory.

⊥ Permanent address: Estacion Experimental Aula Dei (CSIC), Apdo. 3403, 50059 Zaragoza, Spain.

(1) Barber, J. *Q. Rev. Biophys.* **2003**, *36*, 71–89.

(2) Blankenship, R. E. In *Molecular Mechanisms of Photosynthesis*; Blackwell Science: Oxford, 2002; pp 42−123.

(3) Grotjohann, I.; Jolley, C.; Fromme, P. *Phys. Chem. Chem. Phys.* **2004**, *6*, 4743–4753.

(4) Ferreira, K. N.; Iverson, T. M.; Maghlaoui, K.; Barber, J.; Iwata, S. *Science* **2004**, *303*, 1831–1838.

 10.1021/ja908510w

the PSII core complex. Both are responsible for light-harvesting and excitation energy transfer (EET) to the RC. CP43 may also be involved in stabilization of the OEC.[3,5] In turn, CP47 besides its light harvesting and EET functions is believed to play a role in the dimerization of the PSII core.[6−8] The crystal structure of PSII was recently refined to 3.0[9,10] and 2.9 Å,[11] respectively. Both structures revealed that CP43 and CP47 contain 13 and 16 chlorophyll *a* (Chl *a*) molecules, respectively. The RC complex contains six Chl *a* and two pheophytins *a* (Pheo *a*).[9−11]

To provide more insight into the nature of the PSII core complex, it is necessary to understand the nature of its intact isolated components, i.e., core antenna systems CP43 and CP47, as well as the RC. Regarding the isolated CP43 complex of PSII, we have demonstrated recently that this pigment antenna complex has two quasi-degenerate "red" absorption states (A and B). The site distribution functions (SDFs) of red-states A and B are uncorrelated, and narrow holes are burned into subpopulations of chlorophylls (Chls) from states A and B, which are the lowest-energy pigments in their particular CP43 complexes and, thus, cannot further transfer energy downhill. Using the uncorrelated EET model,[12] various optical spectra of the CP43 complex could be well fitted, providing strong evidence for the existence of efficient energy transfer between the two lowest energy states A and B in CP43.[13] We have shown that these results are consistent with the excitonic calculations, which suggest that the best Chl candidates for the low-energy A and B states are Chl 44 and Chl 37 (numbering of Loll et al.[9]), respectively.[14] A somewhat different assignment was proposed by Raszewski and Renger,[15] where it was argued that the three lowest site energies in CP43 belong to Chls 37, 43, and 45.

Regarding the CP47 complex, earlier data obtained at low temperatures showed significant differences between optical spectra of the same type for different samples (vide infra).[16−20] For example, low temperature (4.2 K) fluorescence spectra of the isolated CP47 complex obtained by various groups appeared to be contributed to by at least three different emission bands resulting in variable fluorescence maxima in the range of 690−693 nm.[16−18,21,22] Huyer et al.[23] suggested that the isolated CP47 complex contains two subpopulations having lowest energy states with distinctly different lifetimes (∼1.6 ns and ∼6.2 ns for "fast"- and "slow"-state subpopulations, respectively). The fast-state subpopulation with emission maximum near 685 nm was significantly larger in CP47 sample prepared without a cryoprotectant, and the relative contribution of the 685 nm emission, as observed by various laboratories,[17,18] was sample dependent, signaling possible destabilization of the protein. This motivated us to return to the study of CP47 antenna protein complexes using freshly prepared samples (vide infra).

There are several additional motivating factors for resuming studies of isolated CP47 complexes. First, on the basis of the analysis of hole-burned spectra and the 4.2 K static fluorescence spectra obtained previously, it has been concluded that the lowest energy state of CP47 lies at 690 nm with a fluorescence origin band near 690−693 nm.[16,17,20] This appears to be in disagreement with the 695 nm CP47 emission maximum observed in the intact PSII core complex. Second, in 1995 M.L. Groot et al.,[22] based on the analysis of the triplet-minus-singlet (T-S) spectra, concluded that the lowest lying trap state in CP47 is at ∼685 nm, and this state gives rise to the observed fluorescence origin band at 690 nm. In ref 24, on the other hand, it was assumed that 695 nm emission observed in intact PSII core complex originates from CP47 and is associated with the 690 nm absorption band. This would suggest a large Stokes shift, a questionable assumption as the strength of the electron−phonon (el-ph) coupling in the CP47 is believed to be only moderately strong, with the Huang−Rhys factor $S \leq 1$.[15,17,18] In fact, in 1998 den Hartog et al.[17] showed by HB spectroscopy that the CP47 trap lies near 690 nm and found an S value of ∼0.7 in agreement with the observed 690−691 nm fluorescence origin band.[17,22] Third, in 1997 Polivka et al.[18] suggested that fluorescence of the wild type CP47-D_1D_2-Cyt_{b559} complex could be ascribed to fluorescence of two Chl *a* clusters of CP47 with fluorescence maxima at ∼688 and ∼695 nm. Our analysis of previously published fluorescence spectra showed that all emission spectra consist of two (or more) spectral contributions with relative contributions being sample dependent (see below). In addition, CP47 studies by de Weerd et al.[19] including pump−probe (magic-angle) data ($T = 77$ K) and global analysis fit for CP47 after 670.0 nm excitation showed that one of the species associated difference spectra (SADS) was linked with only a partial relaxation from the Chls that were bleached at 677 nm and 683/684 nm to a Chl absorbing at even lower energy. Though not commented on by the authors, this could mean that in this particular CP47 sample the EET was not very efficient from the 683/684 nm state. The SADS spectra obtained at 17 ps and a few nanoseconds showed the bleach with a peak near 684−685 nm. It appears that the 685 nm peak (asymmetric and very broad, with full width at half-maximum (fwhm) of ∼11 nm) contained a contribution from the 684 nm pigments along with bleaches from 690/695 nm bands. A significant contribution to the discussed SADS spectra from the 684 nm state is consistent with our own observations

(5) Shen, J.-R.; Henmi, T.; Kamiya, N. In *Photosynthetic Protein Complexes*; Fromme, P., Ed.; Wiley-VCH: Weinheim, Germany, 2008; Chapter 4, pp 83−106.
(6) Krausz, E.; Hughes, J. L.; Smith, P.; Pace, R.; Årsköld, S. P. *Photochem. Photobiol. Sci.* **2005**, *4*, 744–753.
(7) Barber, J.; Morris, E.; Buchel, C. *Biochim. Biophys. Acta, Bioenerg.* **2000**, *1459*, 239–247.
(8) Bricker, T. M.; Frankel, L. K. *Photosynthesis Res.* **2002**, *72*, 131–146.
(9) Loll, B.; Kern, J.; Saenger, W.; Zouni, A.; Biesiadka, J. *Nature* **2005**, *438*, 1040–1044.
(10) Müh, F.; Renger, T.; Zouni, A. *Plant Physiol. Biochem.* **2008**, *46*, 238–264.
(11) Guskov, A.; Kern, J.; Gabdulkhakov, A.; Broser, M.; Zouni, A.; Saenger, W. *Nat. Struct. Mol. Biol.* **2009**, *16*, 334–342.
(12) Zazubovich, V.; Jankowiak, R. *J. Lumin.* **2007**, *127*, 245–250.
(13) Dang, N. C.; Zazubovich, V.; Reppert, M.; Neupane, B.; Picorel, R.; Seibert, M.; Jankowiak, R. *J. Phys. Chem. B* **2008**, *112*, 9921–9933.
(14) Reppert, M.; Zazubovich, V.; Dang, N. C.; Seibert, M.; Jankowiak, R. *J. Phys. Chem. B* **2008**, *112*, 9934–9947.
(15) Raszewski, G.; Renger, T. *J. Am. Chem. Soc.* **2008**, *130*, 4431–4446.
(16) Alfonso, M.; Montoya, G.; Cases, R.; Rodriguez, R.; Picorel, R. *Biochemistry* **1994**, *33*, 10494–10500.
(17) den Hartog, F. T. H.; Dekker, J. P.; van Grondelle, R.; Völker, S. *J. Phys. Chem. B* **1998**, *102*, 11007–11016.
(18) Polivka, T.; Kroh, P.; Psencik, J.; Engst, D.; Komenda, J.; Hála, J. *J. Lumin.* **1997**, *72−74*, 600–602.
(19) De Weerd, F. L.; van Stokkum, I. H. M.; van Amerongen, H.; Dekker, J. P.; van Grondelle, R. *Biophys. J.* **2002**, *82*, 1586–1597.
(20) Chang, H.-C.; Jankowiak, R.; Yocum, C. F.; Picorel, R.; Alfonso, M.; Seibert, M.; Small, G. J. *J. Phys. Chem.* **1994**, *98*, 7717–7724.
(21) van Dorssen, R. J.; Breton, J.; Plijter, J. J.; Satoh, K.; van Gorkom, H. J.; Amesz, J. *Biochim. Biophys. Acta, Bioenerg.* **1987**, *893*, 267–274.
(22) Groot, M.; Peterman, E. J. G.; van Stokkum, I. H. M.; Dekker, J. P.; van Grondelle, R. *Biophys. J.* **1995**, *68*, 281–290.
(23) Huyer, J.; Eckert, H. J.; Irrgang, K.-D.; Miao, J.; Eichler, H. J.; Renger, G. *J. Phys. Chem. B* **2004**, *108*, 3326–3334.
(24) Krausz, E.; Hughes, J. L.; Smith, P. J.; Pace, R. J.; Årsköld, S. P. *Photosynth. Res.* **2005**, *84*, 193–199.

over the years that the extent of the triplet-bottleneck hole near 684 nm varied from preparation to preparation[20] and as a result might be contributed to by destabilized complexes.

To clear up some of the above-discussed findings and to explain the significantly red-shifted emission observed in the intact cores, it is important to identify the lowest-energy states of CP47. This can be accomplished via zero-phonon hole (ZPH)-action spectroscopy[13,25,26] and confirmed by resonant and nonresonant hole-burning (HB) and fluorescence line narrowing (FLN) experiments. Thus, in this work, we focus on sample dependent composition of the ZPH-action spectra, the energy of the lowest-energy trap(s), burn fluence dependent fluorescence spectra, excitation energy transfer (EET) between different groups of pigments contributing to different low-energy states, and a variable contribution from transient holes observed near 684 nm. The information on the extent to which the Q_y states are excitonically correlated, i.e., share common Chl *a* molecules, is studied by Monte Carlo simulations in ref 27, where the calculated CP47 absorption, emission, and persistent hole burned (HB) spectra are compared with the experimental results obtained for the native CP47 to provide more insight into the electronic structure of the CP47 complex.

2. Materials and Methods

2.1. Isolation of the CP47 from Spinach. CP47 proximal antenna complex was purified as in refs 16 and 28 with some modifications. The material extracted from the PSII core complex with 7.5% (w/v) dodecyl maltoside (DM) and 2 M $LiClO_4$ was dialyzed against 1 L of a buffer containing 20 mM Bis-Tris, pH 6.0 for 2 h with one buffer exchange after 1 h and loaded onto a Toyopearl TSK DEAE 650s column, equilibrated in the same buffer with 0.03% (w/v) DM. The material that passed through the column corresponded to the CP43 complex, and the green material that remained on the column was washed with two column volumes of the same buffer and then eluted with a 0−175 mM $LiClO_4$ linear gradient in the same buffer. The first eluted green fractions corresponded to contaminant CP29, the second to CP47 complex, and the third to both RC and CP47/RC complexes. The CP47 fractions were dialyzed overnight against 20 mM Bis-Tris, pH 6.0, and 0.015% (w/v) DM and then loaded onto another Toyopearl TSK DEAE 650s column equilibrated with 20 mM Bis-Tris, pH 6.0 and 0.03% (w/v) DM. The bound material was eluted with a 0−175 mM $LiClO_4$ linear gradient. The green fractions that contained RC, distinguished by the distinctive band from Pheo *a* at around 543 nm, were discarded, and those with a maximum at 675 nm and the same absorption at around 500 nm (due to the carotenoid) as that at 620 nm (due to Chl *a*) were combined, dialyzed against 20 mM Bis-Tris, pH 6.0 and 0.03% (w/v) DM, and concentrated. The purity of the CP47 sample was checked by HPLC and size exclusion chromatography. Spectroscopic studies did not reveal any contribution from disconnected Chls characterized by a 670−673 nm emission band. This material then constituted pure CP47 complex. In this work we discuss data obtained for two preparations obtained at different times labeled below as batch #1 (samples 1A and 1B) and batch #2 (sample 2).

2.2. Spectroscopic Measurements. The hole-burning apparatus used is described in. refs 13 and 29−32. Briefly, absorption and HB spectra were recorded with a Bruker HR125 Fourier transform spectrometer at a resolution of either 4 cm^{-1} or 0.5 cm^{-1}. Nonresonant HB was performed with the green 496.5 nm line from a Coherent Innova 200 Ar^+ ion laser. A tunable Coherent CR699−21 ring dye laser (line width of 0.07 cm^{-1}, laser dye: DCM Special (Exciton)), pumped by a 6-W Coherent Innova 90 Ar^+ ion laser, was used for resonant HB. The intensity of the CR699−21 laser beam was stabilized electro-optically (Brockton Electro-Optics Corp., LPC) and was attenuated using a set of neutral density filters. The persistent nonphotochemical HB (NPHB) spectra reported correspond to the postburn absorption spectrum minus the preburn absorption spectrum, with corrected baselines to ensure that the total integral of the HB spectrum is zero (conservative holes). The triplet bottleneck (transient) HB spectra correspond to the absorption spectrum with laser on minus the spectrum with laser off. Transient hole spectra were measured after the persistent HB process had reached saturation. Burn wavelengths, intensities, and times are given in the figure captions. Fluorescence spectra were obtained with an excitation wavelength of 496.5 nm from the Coherent Innova 200 Ar^+ ion laser. Fluorescence was dispersed by a 300-mm focal length monochromator and detected by a PI Acton Spec-10 (1340 × 400) CCD camera. The fwhm spectral resolution for the fluorescence spectra was ∼0.1 nm. For fluorescence measurements, the OD of the samples (at the maximum of the Q_y band) was reduced to 0.1 per 1 cm sample thickness (at the absorption maximum), and the sample thickness was reduced to ∼1 mm to ensure that reabsorption effects were negligible. The same stabilized ring dye laser pumped by the Ar^+ ion laser (see above) was used to generate the FLN and delta-FLN (ΔFLN) spectra. The Huang−Rhys factor (*S*) for phonon sideband was obtained by SHB.[29,31−33] The shape of the phonon sideband was obtained by fitting the pseudophonon hole in the low-fluence 693 nm SHB spectrum and was tested by comparing the calculated ΔFLN spectrum (using the SHB sideband) with the phonon sideband of the experimental 697 nm ΔFLN spectrum.[34] All resonant FLN and ΔFLN spectra were recorded with a resolution of 1.5 cm^{-1} using a PI Acton SpectraPro 2300i triple grating monochromator equipped with the Spec-10 CCD (back illuminated) camera. Special care was taken to minimize scattered light (as described in ref 35), and the spectra were corrected for the wavelength sensitivity of the detection system. The sample temperature was maintained at 4.5 K (unless otherwise specified) using a Janis 8-DT Super Vari-Temp liquid helium cryostat. The temperature was stabilized and measured with a Lakeshore Cryotronic model 330 temperature controller.

3. Results

3.1. Low Temperature Absorption and Emission Spectra of CP47. Normalized (4.5 K) absorption (curves a) and fluorescence spectra (curves b) of the CP47 complex are shown in Figure 1. Frames A and B show spectra obtained for the same batch #1 with slight differences in sample treatment before the low temperature (*T*) experiments. That is, spectra shown in frame A were obtained for freshly prepared protein (diluted with the storage buffer to low OD, i.e., ∼1.2 at ∼675 nm at room

(25) Pieper, J.; Raetsep, M.; Jankowiak, R.; Irrgang, K. -.; Voigt, J.; Renger, G.; Small, G. J. *J. Phys. Chem. A* **1999**, *103*, 2412–2421.
(26) Hughes, J. L.; Prince, B. J.; Krausz, E.; Smith, P. J.; Pace, R. J.; Riesen, H. *J. Phys. Chem. B* **2004**, *108*, 10428–10439.
(27) Reppert, M.; Acharya, K.; Neupane, B.; Jankowiak, R. *J. Am. Chem. Soc.* **2010**, submitted.
(28) Picorel, R.; Alfonso M. Seibert M. Isolation and Purification of CP43 and CP47 Photosystem II Proximal Antenna Complexes from Plants, In *Methods in Molecular Biology—Photosynthesis Research Protocols*, 2nd ed.; Carpentier, R., Ed.; Humana Press, New York, 2009; in press.
(29) Reinot, T.; Zazubovich, V.; Hayes, J. M.; Small, G. J. *J. Phys. Chem. B* **2001**, *105*, 5083–5098.
(30) Sigl, A.; Orrit, M.; Reinot, T.; Jankowiak, R.; Friedrich, J. *J. Chem. Phys.* **2007**, *127*, 084510/1−084510/7.
(31) Jankowiak, R.; Small, G. J. *Photosynth. React. Cent.* **1993**, *2*, 133–177.
(32) Dang, N. C.; Reinot, T.; Reppert, M.; Jankowiak, R. *J. Phys. Chem. B* **2007**, *111*, 1582–1589.
(33) Purchase, R.; Bonsma, S.; Jezowski, S.; Gallus, J.; Koenz, F.; Vöelker, S. *Opt. Spectrosc.* **2005**, *98*, 699–711.
(34) Rätsep, M.; Pieper, J.; Irrgang, K.; Freiberg, A. *J. Phys. Chem. B* **2008**, *112*, 110–118.
(35) Rätsep, M.; Freiberg, A. *J. Lumin.* **2007**, *127*, 251–259.

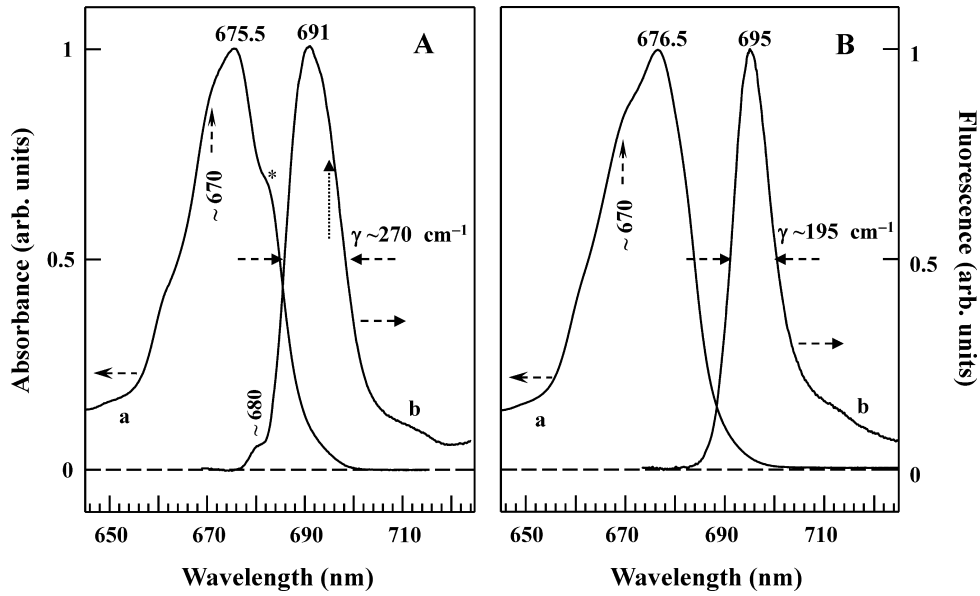

Figure 1. Frames A and B show 4.5 K absorption (curves a) and fluorescence (curves b) spectra of partly destabilized (sample 1A) and intact CP47 (sample 1B). The dashed arrows in frames A and B indicate more absorbance near 670 nm. A more pronounced shoulder near 682−683 nm in frame A is indicated by a star. The dotted arrow in frame A indicates a fluorescence contribution near 695 nm.

Table 1. Summary of the Maxima of Low-Energy States and Nomenclature Used throughout the Paper for Both Intact and Partially Disturbed CP47 Complexes

sample 1A					sample 1B				
	absorption		emission			absorption		emission	
states (intact CP47)	name	$\lambda_{max} \pm 0.3$ nm	name	$\lambda_{max} \pm 0.1$ nm	states (intact CP47)	name	$\lambda_{max} \pm 0.3$ nm	name	$\lambda_{max} \pm 0.1$ nm
1st lowest-E state	A1	~693[b]	F1	695	1st lowest-E state	A1	~693[b]	F1 (major)	695
modified lowest-E state	$A1_{mod}$[a]	[c]	$F1_{mod}$[d]	[d]	modified lowest-E state	$A1_{mod}$	[c]	$F1_{mod}$	[d]
lowest E-traps (destabilized CP47)	name	$\lambda_{max} \pm 0.3$ nm	name	$\lambda_{max} \pm 0.3$ nm					
Trap 1	AT1	689	FT1 (major)	691					
Trap 2	AT2	683.8	FT2	685					
Trap 3	AT3[e]	679.8	FT3	680.3[e]					

[a] In the first approximation one could say that this is the lowest-energy state in CP47 complexes in which the A1 state has been saturated (see Figures 3, 4, and 11 for details), i.e., A1 ceases to be the lowest energy state. However, in reality due to continued HB process the A1 state and resulting fluorescence (see Figures 2B and 3A, respectively) shift blue. $A1_{mod}$ band can be eliminated by temperature cycling while AT1 is not. [b] The maximum of the SDF for the A1 state (SDF_{A1}) lies near 694 nm. [c] The modified lowest energy $A1_{mod}$ state shifts blue as revealed by HB data shown in Figure 2B; for saturated holes this band lies near 688 nm and is similar to that of A2 state of unburned samples. [d] The position of this band due to continued HB also shifts blue, in comparison to band F1; for saturated holes the resulting emission band lies near 692 nm; see Figure 3A. [e] Negligibly small contribution occasionally observed in some samples; see text.

temperature (RT)) and immediately mixed (50/50 *v*/*v* sample/cryogenic solvent) with the cryogenic solvent (i.e., glycerol/ethylene glycol solution; 55/45 *v*/*v*) for future use (no sonication). This sample (labeled below as 1A) was stored in the freezer (−77 °C) for several weeks before use. The absorption spectrum of sample 1A shown in frame A (curve a) is very similar to all CP47 absorption spectra published before.[17,19,20] The corresponding fluorescence spectrum (curve b) shows a broad fluorescence band (fwhm ~13 nm or ~270 cm^{-1}) with a maximum near 691 nm and a weak shoulder near 695 nm (see dotted arrow), in agreement with literature data where the typical fluorescence maximum was observed between 690−693 nm.[16,17,21,22] The large width of the spectrum suggests that the spectrum shown in Figure 1A contain contributions from several fluorescence bands (vide infra). Sonication and/or extended equilibration of samples prepared in this way in darkness did not lead to any measurable changes in the absorption and/or emission spectra.

Spectroscopic assignment of various bands discussed in this work is summarized in Table 1 and will be presented in detail below. Briefly, bands labeled A1/$A1_{mod}$ and F1/$F1_{mod}$ (where the subscript stands for modified) correspond to absorption/fluorescence bands originating from intact CP47 preparations (the $A1_{mod}$ and $F1_{mod}$ contributions are revealed in HB experiments, when the lowest state A1 has already been bleached). Similarly, bands ATX and FTX (with $X = 1$, 2, or 3) correspond to absorption and fluorescence bands originating from destabilized complexes. The weak fluorescence contribution observed in curve b near 680 nm (Figure 1A) labeled as the FT3 was not observed for all samples (in particular, it was never observed for sample 1B), and we ascribe it to a very small subset of perturbed CP47 complexes that cannot transfer energy to lowest energy traps.

We next present the results for the CP47 complex referred to below as sample 1B. This sample (from the same batch as sample 1A) was obtained by diluting the high OD sample (OD

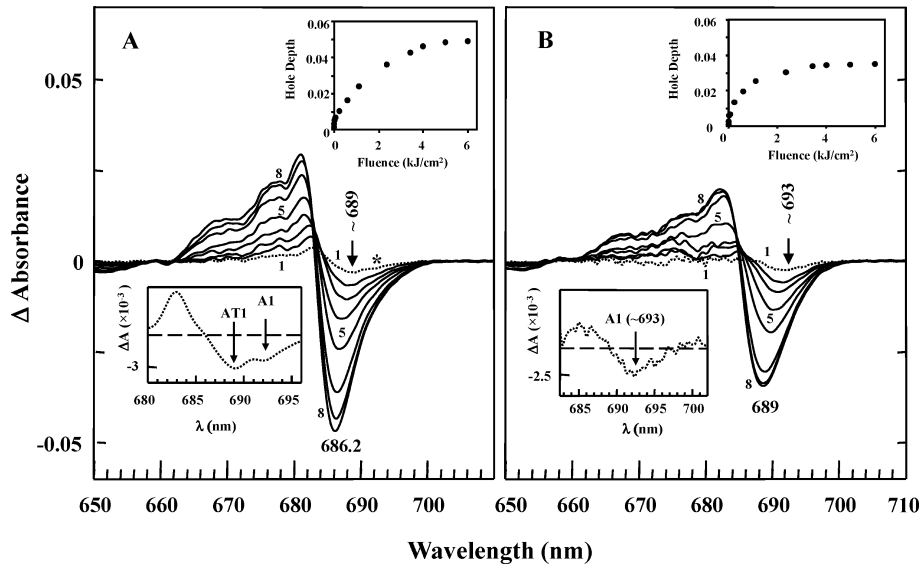

Figure 2. Comparison of nonresonant hole burned spectra obtained with $\lambda_B = 496.5$ nm for samples 1A (frame A) and 1B (frame B). Curves labeled 1−8 (in both frames) correspond to holes obtained for different burn-fluences; the top insets show the inverted hole-depth plotted as a function of fluence. Note that lowest-energy burn states and the minima of the saturated holes in frames A and B are different (see text). The lower left-corned insets in frames A and B corresponds to an expanded curves 1; see text for details.

∼ 20, stored at −77 °C until use) to low OD (∼1.2 near 675 nm at RT) immediately before the experiment; this sample was sonicated and/or incubated in the dark at 4 °C for several minutes and then briefly at RT while mixing with an equal volume of the cryogenic liquid just before the experiment. Note that during storage (i.e., before the experiment) this sample was kept free of cryogenic solvents such as glycerol and ethylene glycol. The absorption spectrum shown in Figure 1B (normalized to 1) is slightly red-shifted with less resolved shoulders in the Q_y-absorption region near 663 and 682 nm and a noticeably weaker absorption near 670 nm. The small red-shift to 676.5 nm is most likely, at least in part, due to a reduced contribution near 670 nm, which is associated with perturbed Chls still residing in protein environment.[22] In addition, from the comparison between absorption spectra in frames A and B (which have the same integrated intensity), it is immediately apparent that the absorption spectrum in Figure 1B shows less resolved contribution near 682 nm, although absorbance in this region is similar. We will argue below that the absorption spectrum shown in Figure 1A is contributed to by partially destabilized CP47 complexes.

The fluorescence spectrum of sample 1B is shown in Figure 1B (curve b). In contrast to the data shown in Figure 1A, the observed emission maximum is red-shifted to 695 nm. The latter is not surprising as we suggested above that the previously published spectra (with maxima near 690−693 nm) must contain other contributions, exhibiting emission near 685 and 690 nm. Both spectra were obtained using low laser power density of 100 μW/cm^2 (with 60-s detection time; fluence (irradiation dose), $f = 0.0060$ J/cm^2). Notably, the fluorescence origin band of curve b in frame B is narrower than that in frame A and has fwhm equal to ∼9.5 nm (i.e., ∼195 cm^{-1}). Thus we believe that this emission band, which we will refer to throughout this paper as F1, corresponds to intact CP47 complexes, especially given that a similar emission band was observed in the PSII core system. To confirm this finding, a second (fresh) batch of CP47 (batch #2) was prepared from spinach for fluorescence studies following the same procedure as that used for sample 1B. It was confirmed that the fluorescence maximum in the new sample was also near 695 nm. We note that in sonicated and equilibrated CP47 samples from both batches the fluorescence maxima of the (0,0)-band and their bandwidths (when obtained for very low fluence, $f = 0.006$ J/cm^2) were independent of the excitation wavelength (λ_{ex}) in the range of 496.5−660.0 nm. We conclude that this red-shifted ∼695 nm emission band (F1) cannot originate from the 690 nm absorption band revealed in refs 17 and 24, as the Huang−Rhys factor (S) associated with the 690 nm band is believed to be relatively small ($S \leq 1$).[15,17,18,20] This calls for a more detailed study of the low-energy excitonic states of the intact CP47 (see section 3.2). To provide more insight into the low-energy Q_y-absorption region both SHB and FLN spectroscopies are used, as discussed below.

3.2. Nonresonant Persistent HB Spectra. NPHB spectra for both samples 1A (frame A) and 1B (frame B) were obtained for several λ_{ex}. We begin with Figure 2, which shows the nonresonantly burned holes (slightly smoothed) using $\lambda_{ex} = 496.5$ nm. Curves shown in frames A and B are labeled as 1−8, and correspond to different fluences. The same fluences (f) were used to obtain curves 1−5 in frames A and B, i.e., $f = 5.2$, 32, 76, 240, and 600 J/cm^2. Different fluences were used to obtain HB spectra labeled as 6, 7, and 8; in frame A: 1844, 2924, and 4004 J/cm^2 and in frame B: 2372, 3444, and 4000 J/cm^2. The arrows indicate the minimum of the broad and shallow hole obtained at the burning fluence of $f = 5.2$ J/cm^2. Similar holes (but more noisy) were obtained for $f = 0.6$ J/cm^2 (not shown). The shallow (low-fluence) holes in frames A and B of Figure 2 (shown as dotted curves and replotted as insets in the lower left-hand corners) are centered at ∼689 and ∼693 nm, respectively. Based on these low-fluence holes, we assign two absorption states A1 (∼693 nm, corresponding to the F1 emission of intact complexes) and AT1 (∼689 nm, corresponding to the lowest state of a subpopulation of perturbed samples and giving rise to a blue-shifted FT1 emission band near 691 nm). While sample 1B shows the presence of only the A1 band, the shallow hole (curve 1) shows both a minor contribution from the A1 band (as indicated by a star in Figure 2A) and a major contribution from the AT1 band. This is more clearly visible in the lower inset in frame A, which shows an expanded curve 1.

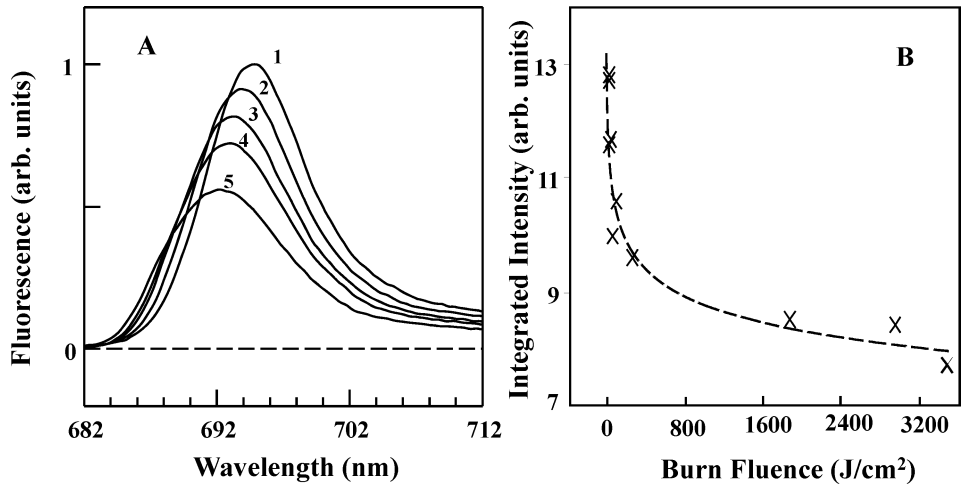

Figure 3. Curve 1 in frame A was the fluorescence (sample 1B) obtained with a very low fluence and shows a maximum at 695 nm. Curves 2−5 in frame A were obtained with the same low fluence after various stages of nonresonant HB; i.e., after burning of hole with different depth. Frame B shows total integrated fluorescence intensity plotted as a function of burn fluence.

These broad holes shift to the blue with higher burning fluence (see curves 8). That is, holes 8 in frames A and B ($f \sim 4000$ J/cm^2) are nearly saturated (see insets in upper right-hand corners) and shifted to about 686.2 and 689 nm, respectively. The fractional OD changes of the holes 1−8 in frames A and B are 3.2−21% and 3.2−31%, respectively. Note that although the absolute depth of the saturated hole (i.e., curves 8) in frame B appears to be smaller than that shown in frame A, its fractional depth is by a factor of ∼1.5 larger than of curve 8 in frame A.

Regarding the broad nonresonant (i.e., non line-narrowed) holes shown in Figure 2B (intact sample), we suggest that these blue shifting holes (curves 1−8) are most easily explained in terms of a gradual modification of the lowest energy state with fluence. At any point during the HB process, the population of CP47 complexes in the sample can be divided into two subpopulations: unburned complexes which give rise to lowest-energy state A1 (as described above) and burned complexes which give rise to a perturbed A1 band which we refer to as $A1_{mod}$. Note that while the A1 band absorption maximum is independent of fluence (although its intensity decreases with time as more complexes are burned) the maximum of the $A1_{mod}$ band both increases in intensity with fluence (as more unburned complexes are burned) and also gradually shifts blue (due to repeated burnings of individual complexes). Since at any fluence complexes contributing to the A1 band have by definition unchanged (unburned) lowest-energy states, they do not contribute to the HB difference spectrum; the blue shift of the HB spectra with fluence is thus entirely determined by (1) the relative population of A1 and $A1_{mod}$ bands (at low fluence, before the A1 state has been entirely bleached) and (2) the spectral position of the $A1_{mod}$ state (at higher fluences, as individual complexes are burned more than once). Considering the entire sample as a whole, then, it is clear that the energy of the lowest state drifts (shifts) blue upon burning depending on the position and relative intensities of the A1 and $A1_{mod}$ bands.

A similar dynamic can be envisioned for sample 1A (Figure 2A), but in this case the description is significantly complicated by the presence of multiple bands, each of which can give rise to its own population of "modified" low-energy states. From the low-fluence hole, it is clear that a major contribution to the sample 1A HB spectrum comes from the AT1 state (corresponding to the lowest energy state of the destabilized CP47 subpopulation emitting near 691 nm (FT1) as already mentioned above), although a smaller contribution from the intact A1 band is also evident. At higher fluences, it appears that the hole is also contributed to by an additional 683.8 nm AT2 band. The latter state (emitting near 685 nm, band FT2) has been observed as a shoulder in emission spectra reported in refs 17 and 18 in this work, its exact position is based on the observation of a triplet-bottleneck HB bleach at 683.8 nm (see section 3.7). The contribution from the AT2 band is also observed in the absorption spectrum shown in Figure 1A (curve a, indicated by a star). We will argue below that the ∼685 (FT2) and ∼691 nm (FT1) emission bands originate from different fractions of CP47 that due to partial destabilization possess different low-energy traps in comparison with intact complex; see sections 3.3 and 4.1.

3.3. Fluence-Dependent Emission Spectra. We turn now to fluorescence spectra obtained at different stages of nonresonant HB. Curve 1 in Figure 3A (sample 1B) shows the emission spectrum obtained with very low fluence (9.6 mJ/cm^2) and is nearly indistinguishable from spectrum b in Figure 1B. Spectra 2−5 were obtained with the same excitation fluence as above but after various stages of nonresonant HB that, as shown in Figure 2B, led to different amount of bleaching and blue shift of HB spectra. Curves 2−5 show that with increasing bleaching the integrated fluorescence intensity decreases and the emission maximum shifts blue to about 692 nm. The integrated fluorescence intensity as a function of HB fluence used to burn nonresonant holes is plotted in Figure 3B. As described above, we believe that spectrum 1 in Figure 3A originates from the lowest-energy state A1 of intact CP47 complexes emitting near 695 nm. The position of this band does not depend on fluence, as long as fluence is kept lower than ∼8 J/cm^2, and is referred to below as band F1. Curves 2−5 shift blue in agreement with HB data discussed above (see Figure 2B). As described above for HB data, this blue shift can be explained assuming that as the pigments contributing to the lowest A1 state are continuously burned, the F1 emission decreases; at the same time the contribution from the blue-shifted $F1_{mod}$ band (originating from the modified low-energy state $A1_{mod}$; see Table 1) increases, and the spectral position of this band changes with fluence. For example, spectrum 5 in Figure 3A is likely to have contributions form both A1 and $A1_{mod}$ states. In other words, the energy and the composition of the lowest-energy state changes continually (due to the continued HB process) leading to a blue shift of the

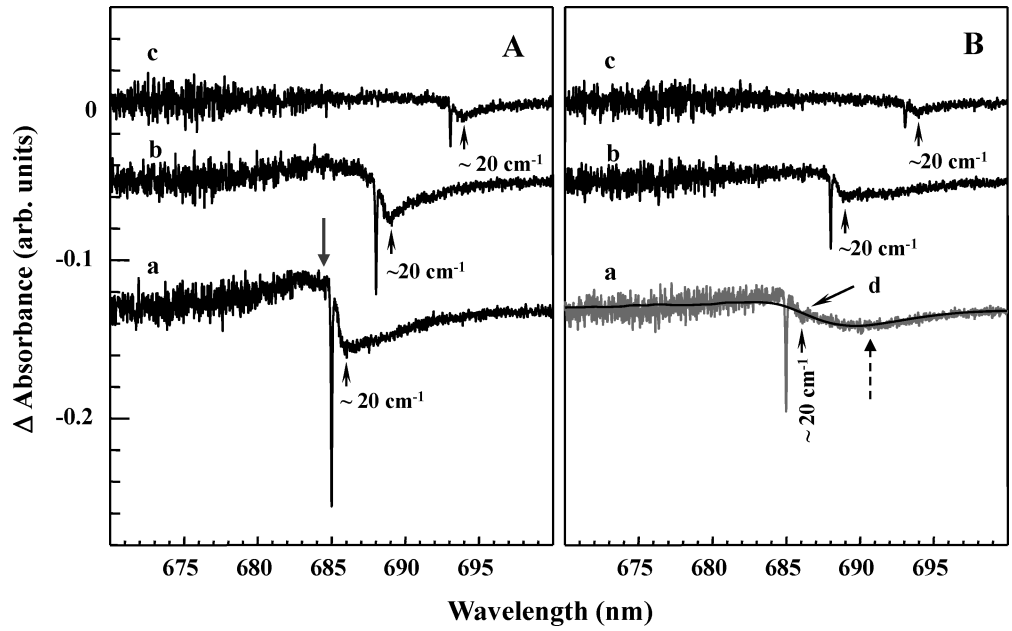

Figure 4. Resonant HB spectra obtained with a constant fluence of 144 J/cm^2 for samples 1A (frame A) and 1B (frame B), respectively. Curves labeled as a, b, and c in both frames were burnt at 685.0, 688.0, and 693.0 nm, respectively. Higher energy excitations (curves a and b) clearly reveal an additional contribution to the pseudophonon sideband hole (compare different shapes/bandwidths of the low-energy holes) due to interference from lowest energy state(s) bleached by downhill EET. Curve d (smooth solid line) is a hole burned spectrum of the same sample burnt with nonresonant excitation at 496.5 nm and a fluence of 600 J/cm^2. The downward solid arrow in frame A (above curve a) indicates the real-PSB hole (see text for details).

resulting emission (which always occurs from the lowest state). Note that the lowest-energy state during the HB process may be contributed to by pigments originally contributing to the first and second-lowest exciton band in unperturbed (unburned) samples. Interestingly, similar dynamics of fluence-dependent emission are also observed in the PSII core from spinach (not shown for brevity). Note that the emission maxima shown in Figure 3 vary more or less in concert with the minima of the nonresonant holes as a function of HB fluence. Thus, in light of the fluorescence spectra shown in Figures 1 and 3 it is not surprising that the maxima of the previously reported fluorescence spectra varied from paper to paper,[16,17,21] if for example different (and much higher[17] or not reported) laser excitation power densities were used to obtain fluorescence spectra (see also discussion of Figure 8). Samples annealed to about 150 K (to erase the holes) provided 695 nm emission at 4.5 K, proving that the process discussed above (i.e., emission shift due to HB process) is reversible. The fluorescence spectra and the dynamics of fully functional Chls in the CP47 complex are further discussed in section 4.1.

3.4. Resonant Persistent Hole Burned Spectra. Figure 4 presents further evidence that the HB characteristics and EET dynamics in samples 1A and 1B are different. Both frame A (sample 1A) and frame B (sample 1B) show persistent NPHB spectra for three different excitation wavelengths (λ_B) in the low-energy region, i.e., 685.0, 688.0, and 693.0 nm. The same burn fluence was used for both samples. The zero-phonon holes (ZPH) plus pseudo phonon sideband (PSB) holes at 20 cm^{-1} from the ZPH are clearly resolved. Again, the difference in the hole-depth and different shape/composition of the low-energy bands is clearly observed in agreement with data shown in Figure 2. In particular, in the case of $\lambda_B = 685.0$ nm (curves a) it is apparent that EET in sample 1A occurs to different low-energy states in comparison to sample 1B, where a more red-shifted and well resolved lowest-energy band is observed. That is, the minimum of the broad (low-energy) hole in the noisy curve a in Figure 4B is near 691 nm (see dashed arrow), and its shape is very similar to the partly saturated hole presented in Figure 2B (curve 5) suggesting that for this burn fluence ($f = 600$ J/cm^2) the lowest-energy state was already partly saturated, and the pigments contributing to the modified lowest-energy state are being bleached. For easy comparison, curve 5 of Figure 2B is replotted in Figure 4B as curve d (dark black line) supporting the above conclusion. This in turn suggests that the lowest-energy state is likely characterized by very low oscillator strength in agreement with low absorbance near 690−695 nm region. The downward solid arrow in curve a (Figure 4A) corresponds to the resolved real-PSB hole at about 20 cm^{-1}.

3.5. Broad-Band Fluorescence and FLN Spectra. To characterize a spectral distribution of the low-energy trap(s), we have performed a series of FLN experiments ($T = 4.5$ K) at different λ_{ex}. Again, all spectra were obtained with very low laser excitation power density (100 μW/cm^2; total fluence used was ~6 mJ/cm^2). The results for samples 1A and 1B are shown in Figure 5, frames A and B, respectively. In agreement with data shown in Figure 1B, a λ_{ex} of 680.0 nm gives a fluorescence maximum near 695 nm (frame B). However, the same λ_{ex} for sample 1A (frame A) provides a slightly red-shifted emission spectrum (i.e., 692 nm) with respect to the broadband fluorescence spectrum of Figure 1A (691 nm). This red-shift can be attributed to a weaker contribution of the FT2 emission band (accessible via the AT2 absorption band at 683.8 nm) combined with a lower degree of bleaching of the A1 state (~693 nm absorption peak). Nevertheless, in this case, state AT1 (i.e., FT1 fluorescence near 691 nm) mostly contributes to the observed fluorescence spectrum. Thus we conclude again that spectrum b shown in Figure 1A originates from both the AT1 and A1 states (i.e., FT1 and F1 emission are observed) with an additional small contribution from the FT2 (see Figure 8A) and FT3 emissions; see section 4.1 and Table 1 for more details. Data shown in Figure 5A illustrate that when λ_{ex} reaches the low-

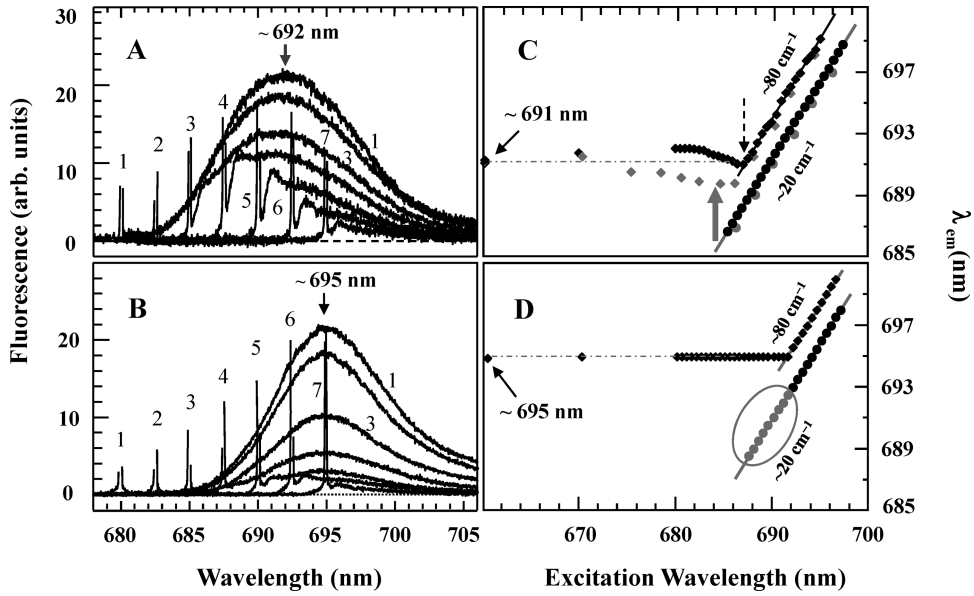

Figure 5. Frames A and B show nonline narrowed and line-narrowed fluorescence spectra obtained for samples 1A and 1B, respectively. Fluorescence spectra labeled 1−7 were obtained using λ_{exc} of 680.0, 682.5, 685.0, 687.5, 690.0, 692.5, and 695.0 nm, respectively. The sharp lines are in part contaminated by a laser scatter and are arbitrarily cut to reveal the nonresonant fluorescence contributions. ΔFLN spectra, however, had negligible contribution from the laser scatter. Frames C (sample 1A) and D (sample 1B) show the positions of the maxima λ_{em} of the fluorescence spectra at 4.5 K as function of λ_{exc}. In both frames (C and D) three types of maxima λ_{em} are plotted. The solid black circle symbols represent the sharp maxima near the 20 cm^{-1} feature from the laser excitation wavelength; in frames C and D the 20 cm^{-1} phonon sidebands are observed for $\lambda_{exc} > 685$ and 687 nm, respectively. The solid black diamond symbols represent the position of the broad fluorescence maximum (i.e., nonresonant fluorescence). In the spectral region where the 20 cm^{-1} mode is observed in addition to the broad fluorescence band, a weak mode near 80 cm^{-1} is also observed as indicated by the solid black diamond symbols (extended spectra and hole shape analyses are not shown for brevity). The curves traced through the data are guides for the eye. In frame C, for comparison, the gray diamonds and circles represent similar data from.[17] Note different depth and width of the "dip" in frame C (see thick gray and dashed arrows in frame C) and its absence in frame D.

energy trap(s) resonant FLN spectra are also observed. Figure 5, frames B and D (data for sample 1B), illustrate that although a low laser excitation power was used, due to multiple spectra obtained for the same sample, a small contribution from the $F1_{mod}$ emission cannot be excluded. Such contribution, however, in intact CP47 can be eliminated by cycling temperature from 4.5 to 150 K and back to 4.5 K (vide supra); this is not the case for the destabilized samples, which independent of temperature cycling always reveal the low-energy trap AT1 and its FT1 emission near 691 nm.

FLN spectra shown in Figure 5A are in agreement with the data reported previously,[17] but as argued below, results shown in Figure 5B correspond to more intact CP47 sample with a majority of complexes undergoing efficient "downhill" EET from higher lying states to the lowest energy trap (A1) near 693 nm. Frame 5B clearly shows that the EET in intact complexes is significantly less disturbed than that observed in frame A for sample 1A. Frames C (sample 1A) and D (sample 1B) show the positions of the maxima λ_{em} of the fluorescence spectra at 4.5 K as function of λ_{exc}. In both frames (C and D) three types of maxima λ_{em} are plotted (see figure caption for details). The intactness of sample 1B is apparent when the data obtained for samples 1A and 1B (see black data points in Figures 5C and 5D) are compared with data obtained for CP47 in ref 17 (gray data points in frame C). Our FLN spectra show that line-narrowing starts at 685 and 687 nm for samples 1A and 1B, as shown in frames C and D, respectively. In agreement with previous data,[17] the 20 cm^{-1} phonon sideband and a broader weak shoulder near 80 cm^{-1} from the excitation frequency are resolved. The 80 cm^{-1} is tentatively assigned to the intermolecular vibrational mode of strongly coupled Chls contributing to the respective low-energy exciton bands. In this region, as expected, the slope $d\lambda_{em}/d\lambda_{exc} = 1$ due to resonant emission; λ_{em} is defined as the maximum of the broad (nonresonant) emission band and/or the maximum of the resolved PSB. The solid lines are guides for the eye. Note that the "dip" near 684 nm observed in ref 17 (see gray diamonds in frame C, as indicated by the gray solid arrow pointing up) is blue-shifted and deeper than that in the sample 1A of this work (see downward dashed arrow); see section 4.4 for discussion.

In intact complexes, in the case where the A1 state is partially burned, the resulting emission also shifts to higher-energies as shown in Figure 3. This means that in a fraction of complexes either a pigment (or a group of pigments) with red-shifted site energies is (are) burned (as illustrated in the fluence dependent emission spectra), leading to higher energy fluorescent traps. This is consistent with the fluorescence spectra further discussed in section 4.1. Interestingly, a contribution from the FT2 emission in our fluorescence spectrum (curve 1 in Figure 5A) is indeed smaller in comparison with data shown in ref 17, in agreement with data shown in Figure 5C. This is why in our CP47 1A sample the dip (see dashed arrow above the black diamonds in frame 5C) is shifted to longer excitation wavelengths with a red-shifted fluorescence origin band, when compared with data from[17] (see gray diamonds). This could suggest, as assumed in 17, that the λ_{em} versus λ_{exc} observed in frame C of Figure 5 is due to a competition between the ~684 nm (AT2) and ~689 nm (AT1) states in the same complex (see Table 1) or as suggested by data reported in this work, such behavior originates from a selective excitation of AT1 and AT2 subpopulations and possible fluence dependent phenomena discussed above. Note that no such dip is observed for sample 1B in frame D of Figure 5, where the majority of emission comes from the A1 state. Note that for $\lambda_{ex} \geq 692$ nm, emission shifts resonantly in the same way in both samples, consistent with both preparations possessing the same lowest-energy band

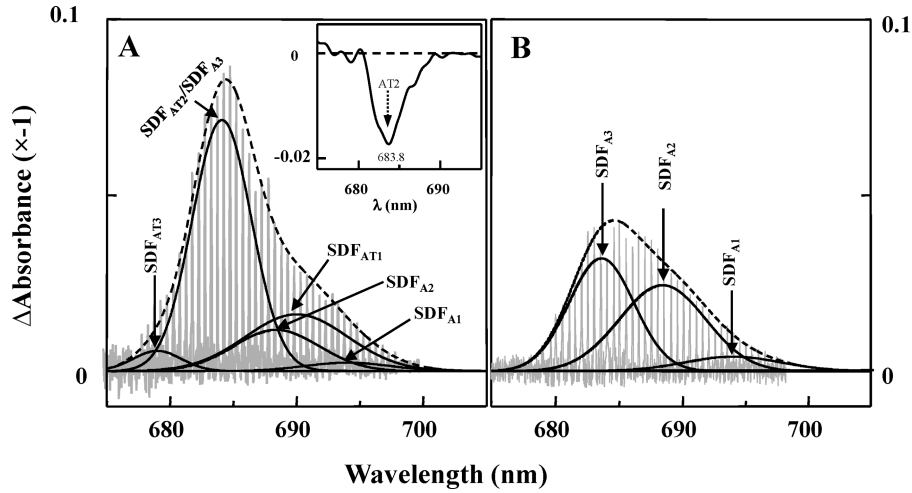

Figure 6. Frames A (sample 1A) and B (sample 1B) show the inverted ZPH-action spectra (see light gray sharp spikes). The dashed lines in frames A and B, respectively, show the sum of the various SDF; the solid lines in frame A are SDF of A1, A2, AT1, AT2/A3, and AT3 (see text for details). Frame A indicates more efficient HB in sample 1A at 683.8 nm (AT2 trap) and 689.0 nm (AT1 trap) in agreement with the observed emission spectra. Frame B shows deconvolution of the ZPH-action spectrum into three Gaussian SDFs with band maxima near 694 (SDF_{A1}), 688.5 (SDF_{A2}), and 683.5 nm (SDF_{A3}).

A1. The only difference between samples 1A and 1B is that sample 1A has additional contribution from the FT1 (∼691 nm) and FT2 (685 nm) emissions. In fact, careful inspection of curve 5 in Figure 5A clearly suggests that this curve is contributed to by nonresonant F1 emission near 695 nm that originates from the intact complexes, i.e., emission from the A1 state. The intensity of the broad shoulder near 695 nm is too strong to originate only from phonons. Thus we conclude that in sample 1B (intact CP47) the majority of complexes are characterized by very efficient EET to the lowest energy A1 trap near 693 nm, resulting in 695 nm emission (F1 band) and negligible emission from the $F1_{mod}$ (as a result of low fluence used). No contribution from the FT1 and/or FT2 bands are observed; see Table 1 for a summary. However, since several fluorescence spectra were generated for the same sample (in a single experiment), in some complexes the A1 state could be already burned, as revealed by the weak contribution from the resonant emission for excitation wavelengths of 687−691 nm; see the 20 cm^{-1} phonons encircled by a gray ellipse (gray circles) in frame D. These very weak phonon sidebands (originating from the resonant emission of the weak $A1_{mod}$ and/or less likely from the AT1 band) are superimposed on the broad F1 emission band centered at 695 nm.

3.6. ZPH-Action Spectra. ZPH-action spectroscopy is another mode for investigating the lowest energy states of CP47. In this spectroscopy, one determines the dependence of the shallow ZPH depth on λ_B under constant burn fluence conditions.[13,26] Different shapes of ZPH-action spectra, obtained for different preparations in absorption mode, have already been published.[20] In ref 20, in absorption mode, two bands were observed at ∼690 and ∼684 nm.[20] Holes burned in the low-energy region were also probed by means of fluorescence excitation with detection wavelength $\lambda_{det} \geq 715$ nm.[17] In this case a broad Gaussian profile was extracted with a maximum at ∼688.9 ± 0.4 nm and a width of ∼200 cm^{-1}. There is a simple explanation for the observed difference in the shape of the ZPH-action spectra depending on the detection mode. That is, in the action spectra measured in fluorescence excitation mode, the states are detected only if they directly or indirectly lead to fluorescence. This could suggest that fluorescence quantum yield of a fraction of complexes with the lowest-energy state near 684 nm (AT2 band) is lower in agreement with ref 23, where it was shown that pigments contributing to the ∼685 nm emission band (FT2) have shorter fluorescence lifetime (∼1.6 ns[23]) than Chls emitting near 690 nm.[23] In addition, under the experimental conditions used in ref 17 (where only the fluorescence emitted at >715 nm was detected), the fraction of light emitted and detected from the AT2 state was significantly smaller than that from the A1 and AT1 bands.

Figure 6, frames A and B, show constant fluence ($f = 10$ J/cm^2; read resolution 0.5 cm^{-1}) inverted zero-phonon HB spectra (i.e., the narrow spikes) obtained for different burn wavelengths in the low-energy region of the CP47 absorption spectrum of samples 1A and 1B, respectively. These profiles suggest that that there are several site-distribution functions (SDF) contributing to the ZPH-action spectra; all holes were burned in the same sample starting from the "red" to "blue" absorption region. In frame 6B, the ZPH action spectrum for sample 1B is plotted together with a suggested decomposition into three Gaussian bands, based on the absorption/fluorescence bands discussed above. The first band, SDF_{A1}, peaks at 694 nm, has a full width of ∼180 cm^{-1}, and corresponds to the phonon-free distribution function of the A1/F1 absorbing/fluorescing states (note that 694 as expected is approximately the average of the A1/F1 peak positions). In addition to this expected band, two additional Gaussian distributions were required to fit the ZPH action spectra. The first band, denoted SDF_{A2}, peaks at 688.5 nm and carries a width of 160 cm^{-1}; the second, SDF_{A3}, peaks at 683.5 nm with a width of ∼120 cm^{-1}. As discussed above, the SDF_{A1} (694 nm) state is the major fluorescent state in sample 1B. The appearance of the two higher-energy bands may at first appear puzzling since in an intact sample at low fluence HB is expected to occur only in the lowest energy A1 state. We suggest that these bands may be present for two reasons, one experimental and one theoretical. First, since ZPHs were measured in our experiment from red to blue, by the time we reach these bands the A1 state in many complexes may be already burned so that hole burning occurs in the modified $A1_{mod}$ state (note that the lowest-state photoproduct lies in this region, see Figure 2B, low fluence holes). Second, from a more theoretical standpoint, these bands may have an excitonic origin, indicating coupling between the lowest state and higher frequency states absorbing in the SDF_{A2} and SDF_{A3} absorption ranges. This excitonic explanation is supported by our recent

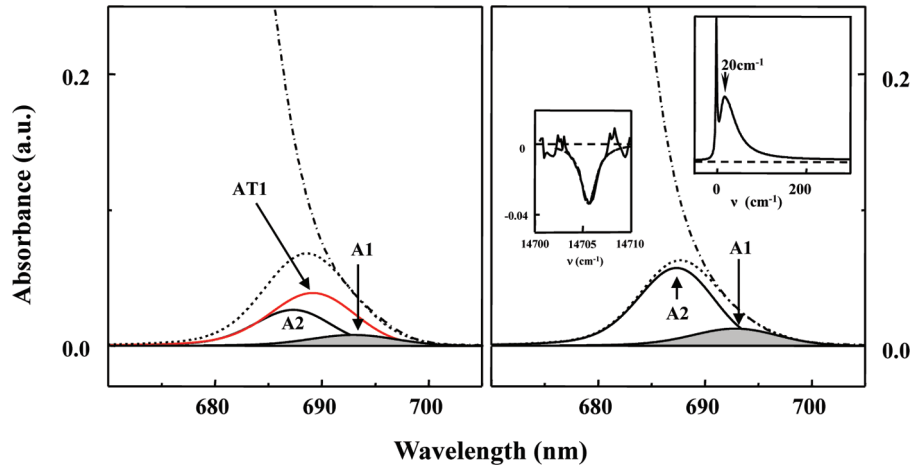

Figure 7. Fit of the low-energy side of the absorption spectra (dot-dashed curve) of sample 1A (frame A) and sample 1B (frame B) using the SDF_{A1} and SDF_{A2} bands (from Figure 6B) convoluted with a single site absorption (SSA) spectrum shown in the upper inset of Figure 7B. The intensity of these bands (using the same ratio) was adjusted to fit the low-energy side of the absorption spectrum. The SSA spectrum was obtained using SHB data; the lower inset in frame B show the ZPH burned at 680.0 nm and its Lorentzian fit (see text for details).

theoretical exploration of the effects of excitonic interactions on nonresonant NPHB spectra,[36] although a detailed description of excitonic effects in resonant HB spectra has not to our knowledge yet appeared. In either case, for our present purposes, they can be regarded in approximate sense as indicative of higher energy absorption states in CP 47.

The holes burned in sample 1A (Figure 6A) have a much different ZPH action profile with deeper holes (using similar fluence) burned in the 682−686 and 688−692 nm regions. Holes burned in this spectral range, in addition to identical input from intact CP47 complexes (see Figure 6B) originate from destabilized complexes with the corresponding SDFs near 684 (SDF_{AT2}) and 690.0 nm (SDF_{AT1}). Thus in sample 1A holes are preferentially burned in the AT1 and AT2 bands in perfect agreement with the observed additional emission bands near 691 and 685 nm; see Figure 8A. Although the assignment of contributions from various states is significantly more complicated in this sample due to the presence of multiple low-energy traps, one feasible fit with Gaussian bands is shown in frame A. The inset in Figure 6A shows a transient hole (sample 1A) originating from the AT2 band; see section 4.6 for details.

Finally we note that the hole width in both frames increases at shorter wavelengths due to EET to the lowest-energy trap(s). Although the width of the holes of the lowest-energy SDF_{A1} band is ultimately limited by the spectrometer resolution of 0.5 cm^{-1}, it is discernible that the holewidths obtained at 680.0 and 683.0 nm for intact sample 1B (after correction for resolution) were about 2 and 1.7 cm^{-1}, respectively, which based on eq 1 correspond to ∼5 and ∼6.5 ps EET time to the lowest trap near 693 nm.

$$\Gamma_{hom} = (1/2\pi cT_1 + 1/2\pi c\tau_{EET}) + 1/\pi cT_2^* \approx 1/2\pi c\tau_{EET} \quad (1)$$

where Γ_{hom} is the homogeneous line width (half-width at half-maximum), T_1 is the fluorescence lifetime, T_2^* is the "pure" dephasing time, and τ_{EET} is the excitation energy transfer time.[33] As an example, the lower insert in Figure 7B shows the hole shape burned at 680.0 nm along with a Lorentzian fit with fwhm of ∼2 cm^{-1}. A similar holewidth (∼1.8 cm^{-1}) was observed for sample 1A.

Figure 7 shows the three approximate absorption bands A1, A2, and AT1 (frame A) and bands A1 and A2 (frame B) that were obtained by convoluting SDF_{A1}, SDF_{A2}, and SDF_{AT1} shown in Figure 6 with the single-site-absorption (SSA) spectrum shown in the upper inset of Figure 7B. For simplicity the same SSA spectrum was assumed for all three states. This spectrum was obtained by fitting the pseudophonon hole of the 693 nm SHB spectrum (Figure 4, curve c of frame B) with a Gaussian (23 cm^{-1} fwhm) on the low-energy side and with a Lorentzian (60 cm^{-1} fwhm) on the high-energy side of $\omega_m = 20$ cm^{-1}. The SSA spectrum was generated from this curve by adding a narrow Lorentzian function with proper scaling to reproduce a Huang−Rhys factor of $S = 1$ (obtained from fluence-dependent SHB at 693 nm, data not shown for brevity). The obtained SSA spectrum was checked by comparing the calculated ΔFLNS[34] phonon sideband using this curve with the experimental spectrum measured for 697 nm excitation (data not shown). With a mean phonon frequency $\omega_m = 20$ cm^{-1} for sample 1B, the Stokes shift between the absorption and fluorescence origin (for weak el-ph coupling) is expected to be $2S\omega_m \sim 40$ cm^{-1},[37] in agreement with the experimental reorganization energy measured by the shift between the A1 and F1 bands. (The estimated S value included the weak contribution from the 80 cm^{-1} phonon modes). The sum of curves A1 and A2 in Figure 7B and A1, A2, and AT1 in Figure 7A (with adjusted intensities) fit very well the low-energy wing of the absorption spectra of samples 1B and 1A (dashed-dotted lines in frames A and B). The fits are in excellent agreement with the shape of the low-energy absorption tails. The oscillator strengths of the lowest-energy A1 and A2 states in this fit are 0.2−0.3 Chl and ∼0.8 Chl, respectively. Thus, in the first approximation, these two low-energy bands correspond to the two lowest excitonic states A1 and A2 of intact CP47, although we emphasize that the parameters of the A2 state should be regarded only as approximations since they are based largely on fits to the ZPH action spectrum, which as discussed above is somewhat difficult to interpret. These states exist in both CP47 samples discussed above with the major difference that sample 1A has a large

(36) Reppert, M.; Naibo, V.; Jankowiak, R. *J. Chem. Phys. B* **2009**, *131*, 234104.

(37) Hayes, J. M.; Gillie, J. K.; Tang, D.; Small, G. J. *Biochim. Biophys. Acta, Bioenerg.* **1988**, *932*, 287–305.

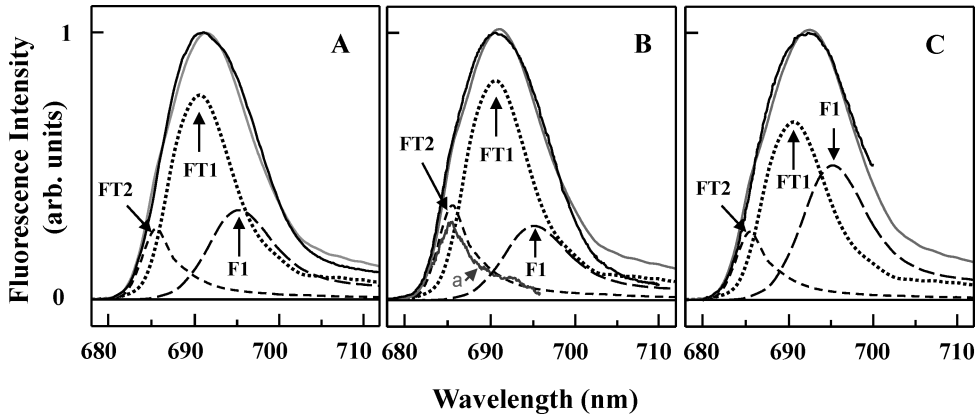

Figure 8. Broad band fluorescence spectra (solid lines) of various CP47 samples. Frame A shows results of an analysis of the emission spectrum for sample 1A (the minor FT3 contribution near 680 nm was subtracted and only F1, FT1, and FT2 contributions remained). Frames B and C describe the composition of fluorescence spectra from refs 17 and 18, respectively. Deconvolution shows that these spectra can be also fitted with the same three major contributions: (i) FT2 with maximum near 685 nm, (ii) FT1 near 691 nm, and (iii) F1 emission with a maximum near 695 nm; see text for details.

additional contribution from the AT1 and AT2 bands as shown in Figure 6A. The ratio of band A2 to band A1 in both absorption spectra in Figures 6 and 7 are the same. Note that, as expected, there is no emission from the A2 band in intact (not burned) samples.

3.7. Triplet Bottleneck Transient Holes. Now we turn to the nonresonantly burned transient hole which, by the nature of the transient HB process, is free from photoproduct contribution. As before,[20] a broad hole at 683.8 nm (obtained with excitation wavelength of 496.5 nm ($I_B = 200$ W/cm^2) was clearly observed in sample 1A as shown in the inset of Figure 6A. The absorbance change at 683.8 nm was ~5%. Interestingly, this hole (for the same fluence) was absent in sample 1B. This is not surprising, as we have noticed over the years that the depth of transient holes in CP47 was dependent on preparation, with shallower holes observed in more recent samples. Thus we suggest that in unperturbed CP47 complexes (due to efficient EET to the lowest energy trap near 693 nm and lack of the AT1 and AT2 traps from the destabilized complexes) such holes should not be observed.

It has been previously argued that the diminution of the intensity of the ~684 nm transient hole was accompanied by increased absorption at ~670 nm.[20] We do not see such correlation in our current preparations; as a result, we conclude that the correlation observed in ref 20 was accidental, as sample 1B has relatively less absorption near 670 nm and no contribution from a transient 684 nm hole. This is in contrast to ref 20 where anticorrelated contributions from the increased absorbance near 670 nm and the transient 684 nm hole were observed. (It should be noted that none of the samples studied in this work showed contribution from a transient hole near 670 nm, demonstrating that the samples studied in this work were not contaminated by free Chls as were many samples studied previously.[17,20−22])

4. Discussion

Taken as a whole, the data presented in the preceding sections establish that sample treatment/preparation is very important for understanding the nature of the electronic structure and dynamics in intact CP47. This is not surprising as minor changes in Chl protein environment are well reflected in low-T optical spectra. Another important finding is that emission of isolated intact CP47 is much narrower (fwhm ~9.5 nm) and located at 695 nm, and not at 690−693 nm (with fwhm ~13−20 nm) as previously reported in a number of papers.[17,21,22] Knowledge of the extent to which destabilized complexes contribute to absorption, emission, and HB spectra is essential before we understand the nature of intact CP47. In what follows we consider first the previously published fluorescence spectra of CP47 and the position/bandwidth of the lowest energy trap(s). This is followed by further discussion of the nonresonant and resonant HB spectra with emphasis on the low-energy absorption region and fluence dependent fluorescence spectra.

4.1. Assignment of the Fluorescing States. In this subsection we continue discussion of relevant literature data related to the fluorescence properties of CP47, in order to provide more insight into the composition of previously published fluorescence spectra. Solid black lines in frames A−C of Figure 8 show a typical low-fluence 4.5 K fluorescence spectrum (frame A) obtained in this work for samples 1A, 1.2 K fluorescence spectrum taken from[17] (frame B), and 4.2 K fluorescence spectrum from[18] (frame C), respectively. Spectra in frames A and B are for the isolated CP47, whereas the experimental spectrum shown in frame C is the emission of CP47-D_1D_2-Cyt b_{559} complex obtained from *Synechocystis* (see Figure 1 in ref 18). Note that all these spectra are very broad with fluorescence maxima in the range of 690−693 nm. Assuming that the fluorescence spectrum shown in Figure 1B (with maximum at 695 nm; F1 band) corresponds to intact complexes, the broad spectra shown in frames A−C must also contain contributions from FT1 and FT2 bands, as already mentioned above (see also table 1). As shown in Figure 8 this is indeed the case, as all fluorescence spectra could be fitted by the F1 (695 nm band), FT1 (691 nm band), and FT2 (685 nm band) contributions by simply adjusting their relative intensities. The sum of these contributions is shown as a gray line. This could indicate that some states are not totally efficient in transferring energy to the lowest-energy A1 state, although a more likely interpretation is, as discussed above, that the samples in question contain contributions from two more subpopulations of complexes in addition to the F1 emission (from intact CP47). Note that a possible contribution of HB to the experimental emission spectra shown in Figure 8, frames B and C, cannot be assessed as no fluence information was provided in refs 17 and 18. Finally, our above assignment of the FT2 contribution is further supported by the shape of the dark gray spectrum (curve a in Figure 8B) that was obtained as a difference between the experimental fluorescence spectra shown in frames A and B of

Figure 8. In addition, sample 1A when kept in the freezer for an extended period of time also revealed more FT2 emission (data not shown). The fact that emission with the origin band near 685 nm (FT2) contributes to the total fluorescence spectra shown in frames A−C of Figure 8 is also consistent with observation by de Weerd et al.,[38] who concluded (based on the changing of the anisotropy of the emission) that the ∼683/684 nm state in their CP47, at least in part, contributed to the 4 K emission. However, in ref 38 it was assumed that a part of the 683/684 nm state would fluoresce and the other part of the same state would transfer energy to the 690 nm pigment, while in our interpretation, the emission near 685 (FT2) and 691 nm (FT1) using low fluence excitation originates from fractions (subpopulations) of CP47 complexes in which the lowest energy traps lie at energies corresponding to ∼684 nm (AT2) and ∼689 nm (AT1), respectively (either as a result of sample perturbation during isolation/preparation, i.e., AT2 band, or as a result of the lowest-energy A1 state being saturated, i.e., burnt away during experiment). Thus, we conclude that data shown in Figure 8 are consistent with HB data discussed above and support our findings that many previously studied samples contained fractions of destabilized and/or photodamaged CP47 complexes.

Finally, for completeness, we comment on the emission spectra shown in ref 16 where it was reported that the emission band of isolated CP47 at 77 K lies at 695 nm. It is interesting to note that the experimental emission spectrum actually plotted in ref 16 appears to show a fluorescence maximum at 692−693 nm (fwhm of ∼24 nm), rather than at 695 nm, possibly suggesting that the emission peak for this preparation depended also on samples conditions, although such an effect was not commented on in that work. In any case, the width of our 77 K spectrum (data not shown) is by a factor of two narrower with fwhm of only ∼12 nm. This is consistent with the analysis presented in Figure 8 as the spectrum in question (from ref 16) could also be deconvolved using F1, FT1, and FT2 contributions (not shown for brevity). Interestingly the fwhm of the 77 K steady-state fluorescence spectrum of CP47 reported in ref 22 was in-between, ∼16 nm, further supporting our findings that previously studied CP47 samples are composites of intact and partly destabilized complexes.

Thus our findings suggest that the previously established pathways for EET in the core light harvesting complex CP47 of PSII[19] most likely do not describe the EET in intact CP47, and more work needs to be done before energy transfer dynamics in intact CP47 protein complexes are well-understood. We conclude that CP47 is more susceptible to destabilization than the CP43 from the PSII core. The conclusion that sample 1A has three emitters, i.e., F1, FT1, and FT2 (with possible contribution from $F1_{mod}$, if high fluence was used for excitation), is also consistent with earlier observations; for example, transient absorption data[19] obtained at 77 K indicated that only part of the 683/684 nm band relaxed to ∼690 nm Chls, suggesting that this band might contribute to the emission spectrum (see section 4.5). By the same token, the 4.2 K fluorescence spectra shown in ref 22 with larger width of the nonselectively excited fluorescence spectra (i.e., fwhm ∼ 12.5 nm versus fwhm of ∼9.5 nm (this work)) also support the idea of several emitters are present in samples with absorption spectrum similar to spectrum a in Figure 1A. A small contribution from the ∼685 nm emission was previously explained by the idea that, due to inhomogeneous broadening of the absorption bands, "683" Chls must exist that are in fact further to the red than the "690" nm pigments.[38] On the basis of the shapes (bandwidths) of the emission spectra in ref 17 and 22, we find this suggestion highly unlikely. Indeed, it should be emphasized in this regard, that such static disorder can result only in narrowed and red-shifted emission spectra, compared with the SDF of the lowest-energy state/pigment in the complex. As a result, as long as all states are coupled by efficient energy transfer, such effects can never produce broadened or blue-shifted spectra such as those observed for sample 1A. In addition, we have found no evidence for this scenario, since in our best CP47 samples, there is no emission with a maximum near 685 nm and the contribution from the band near 690−692 nm (obtained for low fluence) is also absent. Thus, we propose that Chls in intact CP47 are connected via efficient excitation energy transfer to the lowest-energy trap (A1) at 693 nm and that the fluorescence maximum in isolated intact CP47 is at 695 nm (F1 band) and not near 690−693 nm, as previously reported in numerous papers.[17,21,22] The results discussed in this article clearly demonstrate that CP47 antenna−protein complexes should be stored in the absence of glass-forming agents such as glycerol and ethylene glycol. At the beginning of an experiment, the CP47 sample should be gently sonicated for several minutes in a cold buffer, then briefly incubated at 4 °C and subsequently for about 2−3 min at room temperature in the dark, and only then mixed with cryoprotectant shortly before use.

At this point we should mention that site-directed mutations have been introduced to replace conservative histidine residues in CP47.[39] Certain specific mutations can shift the 695 nm emission band in the intact PSII core system to wavelengths between ∼693 and 690 nm.[39] It is important to note here that the mutant results are difficult to interpret for a number of reasons. That is, in view of the data presented in this work, it is difficult to judge to what extent, if any, such shifts might be related to mutations or actually to different experimental conditions (e.g., different fluences or sample preparations) during measurement of fluorescence spectra (particularly since excitation power densities were not reported previously[39]). Our results emphasize once again the extremely sensitive nature of the relationship between protein conformation and electronic spectra; it is thus possible that the spectral shifts observed previously[39] were due to global protein conformational changes or misfolding rather than point-specific changes affecting only the lowest-energy state Chls. Finally, mutations in a number of Chl ligands in CP47 were not studied in ref 39 since at that time these residues had not yet been identified as Chl ligands. This issue is further discussed in ref 27, where the results of excitonic calculations and possible assignments of pigments contributing to the A1 and $A1_{mod}$ excitonic states are also discussed.

4.2. Absorption, HB Spectra, and the Assignment of the Lowest-Energy Absorption State in Intact CP47. To support the data discussed above, we further explored the nature of NPHB spectra obtained for both types of CP47 samples studied in this work. As discussed above, the nonresonantly excited (λ_B = 496.5 nm) NPHB spectra shown in Figure 2 reveal rapidly populated low-fluence holes near 689 nm (frame A, sample 1A) and 693 nm (frame B, sample 1B) by EET from higher-energy states. ZPH-action spectra establish that these broad low-energy states are inhomogenously broadened. At low fluences, these spectra are interpreted in terms of bleaching a single band (the

(38) de Weerd, F. L.; Palacios, M. A.; Andrizhiyevskaya, E. G.; Dekker, J. P.; van Grondelle, R. *Biochemistry* **2002**, *41*, 15224–15233.

(39) Shen, G.; Vermaas, W. F. J. *Biochemistry* **1994**, *33*, 7379–7388.

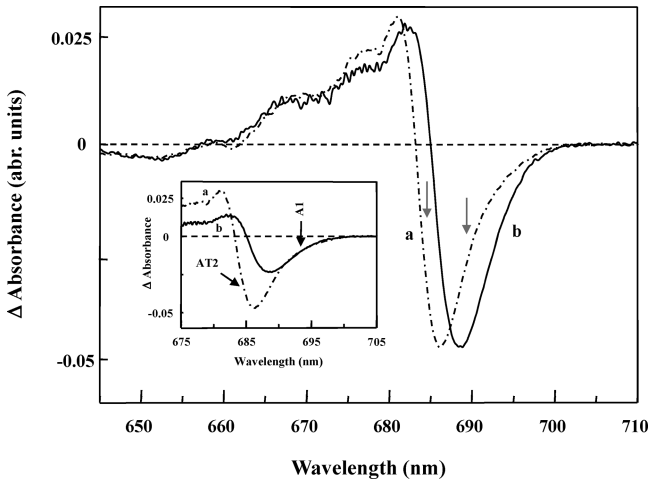

Figure 9. Comparison of the saturated HB spectra from sample 1A (dashed-dotted curve a) and sample 1B (solid curve b) burned at 496.5 nm with a burn fluence of about 4000 J/cm^2 and normalized for same hole depth. The gray arrows from left to right indicate contribution from the AT2 and AT1 traps in sample 1A. The inset shows normalized HB spectra a and b normalized on the low energy side; see text.

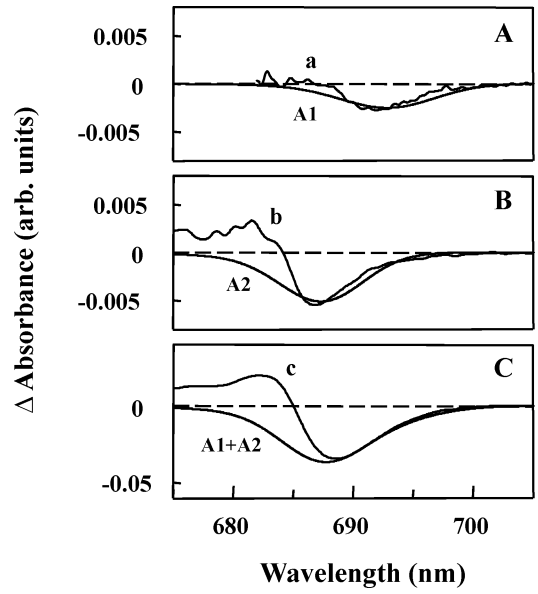

Figure 10. Frames A and B show a comparison of the lowest energy bands A1 and A2 from Figure 7 with various nonresonant HB spectra corresponding to selective bleaching of these two states. Curve a is the low-fluence hole reflecting preferential HB into the lowest-energy A1 state near 693 nm. Curve b is the difference between curves 8 and 6 from Figure 2B, which corresponds to bleaching of the A2 state after saturation of the 1st excitonic state (A1). Frame C shows the sum of A1 + A2 and its comparison to curve c, the saturated HB spectrum (curve 8) from Figure 2B (see text).

~693 nm A1 absorption state), corresponding to the 695 nm F1 emission in sample 1B and bleaching multiple bands in sample 1A (a major contribution from the AT1 state at 689 nm with a smaller contribution from A1). As discussed above, we suggest that the AT1 band is the lowest energy absorption state of a subpopulation of destabilized CP47 complexes in sample 1A and is responsible for the FT1 emission observed near 691 nm.

At high fluences, the NPHB spectra of both samples are contributed to by bleaching of higher-energy absorption states, leading to a blue shift of the modified low-energy state. The different characteristics of the two samples are clearly revealed by comparing the saturated (and normalized to the same hole depth) HB spectra (i.e., curves 8 from Figure 2, frames A and B) obtained for samples 1A and 1B, replotted for convenience as curves a and b in Figure 9. Note the significant blue-shift between the maximum depths of the two saturated spectra, reflecting the large contribution in sample 1A from the blue-shifted states AT1 and AT2. From these two spectra it is very clear that the saturated NPHB spectrum for sample 1A has a significant contribution from the AT2 trap as illustrated in the inset where the two spectra are normalized on the low-energy side. We propose that the presence of the AT2 trap (revealed by the transient hole at 683.8 nm) is responsible for the FT2 emission at ~685 nm, which originates from a fraction of destabilized CP47 complexes. This behavior is also consistent with the different ZPH-action spectra shown in Figure 6.

It is interesting to note that the Δ-absorbance increase in the NPHB spectra measured for both samples is distributed at various wavelengths well beyond the inhomogeneous widths of lowest energy bands and is strongly sample dependent. This suggests that the lowest-energy Chls in both types of CP47 studied in this work are excitonically coupled since the broad antihole observed in Figure 2 can be explained in terms of excitonic interactions between various states as recently demonstrated for excitonically coupled Chls in the CP43 complex[14] and a model excitonically coupled dimer.[36] Excitonic simulations of the low-fluence (sample 1B) HB spectrum, along with other spectra presented in this work, are described in ref 27, where they are used to further explore excitonic interactions in CP47 and potential candidates for the Chls contributing to the lowest energy states.

Finally, frames A and B of Figure 10 compare the nonresonant persistent holes with the shapes of the A1 and A2 bands (from Figure 7). Figure 10A shows that our nonresonant HB spectrum a (taken from Figure 2B, curve 1) is (on low-energy side) in good agreement with the shape of the lowest-energy exciton A1 band. Frame B shows a similar comparison between the second band A2 (from Figure 7) with curve (b) that corresponds to the difference between spectra 8 and 6 of Figure 2B. The latter difference spectrum (curve b) more clearly reflects the bleach of the A2 state in agreement with the observed blue-shift of broad nonresonant holes shown in Figure 2B. Similarity between curves (a) and A1 and (b) and A2 on the low energy side is apparent. The discrepancy on the high energy side is due to the interference from the antihole typically observed in HB experiments. Finally, frame C of Figure 10 shows a comparison between the sum (A1 + A2) bands of Figure 7 and the saturated hole (curve c), which is the same as curve 8 from Figure 2B. These data more clearly illustrate that the extent of the blue shifting with increasing burn fluence is due to saturation of the lowest-energy A1 state and subsequent burning of the A2 state (and higher-energy states at high fluence). We emphasize that in this description HB always occurs on the lowest energy state (A1 or $A1_{mod}$) in the complex. The composition of this state, however, gradually changes; at low fluence it is exactly the A1 absorption state, while at high fluence it comes to reflect properties of higher states (A2, A3, etc.).

The broad low-energy bands in resonant NPHB spectra (λ_B = 685 nm) shown in Figure 4 are also consistent with this analysis. The top HB spectra show only the ZPHs along with the phonon sideband holes, while the shape of the broad holes (to the right of the ZPH) obtained for excitations at 685.0 and 688.0 nm in Figure 4 are very different due to contribution from burning in various absorption states and/or nonresonant burning due to EET. Depending on the sample (see frames A and B of Figure 4), one can see very different shapes and intensities of

the broadband located at lower energies. Disentangling the contributions of phonon-wing absorption and nonresonant HB due to EET is in general very difficult, but it is worth noting that the much stronger phonon-sideband observed for sample 1A in the 685 and 688 nm HB curves is consistent with less efficient energy transfer and/or blue-shifted trap states in this region due to contributions from destabilized complexes.

4.3. Comments on the Total Dephasing Time (T_2). In view of the above results and discussion, we consider briefly the widths of the ZPH burned at 680.0 nm. In both samples the ZPH width at 680.0 nm was about 2 cm^{-1}, providing an EET time (see eq 1) τ_{EET} of ~5 ps, assuming that the contribution from the pure dephasing is negligibly small for $\tau_{EET} \ll T_2$. Detailed analysis of high-resolution holes is beyond the scope of this paper and will be addressed elsewhere. Here, we only mention that τ_{EET} at 684.0 nm (i.e., ~6.5 ps) is slightly faster than that observed previously for the so-called "best" CP47 complex, i.e., sample CP47 (I) in ref 20, where the observed EET time was about 9.5 ps. Interestingly, our ~6.5 ps time constant deduced from the width of the ZPH at 684 nm (data not shown) is faster than the 17 ps component pump−probe data and global analysis fit and SADS spectra connecting lifetimes resulting from the global fit.[19] As in a previous interpretation,[19] we assign this process to an energy transfer event, although the EET time in intact complexes is faster than previously observed.[20] These results suggest that more high resolution HB data and pump−probe experiments on the same intact CP47 samples need to be performed to reveal more details of the EET dynamics in intact CP47.

4.4. Fluorescence-Line Narrowed Spectra, Sample Dependent Trap Pigments, and EET Dynamics. Taken as a whole, the data presented in Figures 5 and 6 establish that the identification of various subsets of CP47 complexes is very important for understanding the nature of intact CP47 antenna protein. Note that in the previously studied CP47 (with absorption spectra similar to that shown in Figure 1A, curve a), the fluorescence anisotropy reached the theoretical value of 0.4 only near 696.9 nm. It is well-known that this can be accomplished only when the absorbing and emitting dipoles are oriented parallel (i.e., there is no energy transfer).[38] This is in agreement with our data shown in Figure 5D, which shows that only for $\lambda_{ex} > 696$ nm is a "pure" ZPL clearly observed with a well resolved phonon sideband (PSB) and no signatures of EET. The fact that well-resolved phonon sidebands about 20 cm^{-1} from the ZPLs are also observed in the 687−692 nm excitation region is consistent with data shown in Figure 6B, where a small contribution from the $F1_{mod}$ band is also present (vide supra). Similar behavior is observed for sample 1A (Figure 5C), in agreement with data presented in ref 17, but in this case there is more contribution from resonantly excited Chls at higher energies (in particular in ref 17 where a relatively larger contribution from the FT2 emission was clearly observed (see Figure 8B).

The interpretation that previously studied CP47 samples[17,21,22] contained one or more destabilized subsets of CP47 complexes is most clearly visible when the black diamonds (sample 1A; this work; see above for details) and the gray diamonds (data from ref 17) in frame C of Figure 5 are compared with data presented in frame D of the same figure. (Recall that the solid black circle symbols represent the sharp maxima near the 20 cm^{-1} feature from the laser excitation wavelength; in frames C and D the 20 cm^{-1} phonon sidebands are observed for $\lambda_{exc} >$ 685 and 687 nm, respectively. The solid black diamond symbols represent the position of the broad fluorescence maximum (i.e., nonresonant fluorescence)). That is, frame C shows that in these samples emission originates from selectively (i.e., resonantly) excited pigments within three respective low-energy traps (i.e., A1, AT1, and AT2), with the AT1 and AT2 traps blue-shifted. Note that the extent of the "dips" (see the gray and dashed arrows in frame C) is sample dependent. That is, as discussed above, the AT1 and AT2 traps clearly contribute to the observed emission spectra in frame A of Figure 5. A very weak contribution from the resonant $F1_{mod}$ or FT1 emission in sample 1B in Figure 5D (indicated by the gray ellipse) is also consistent the analysis presented above. We do not concur with the explanation of ref 17 that the dip occurs because of the presence of competing traps in the same complex. Rather, we believe that the extent of the dip (and different behavior shown in frames C and D) is caused by (i) the relatively larger contribution from destabilized complexes in sample 1A (trap AT2 emitting near 685 nm) and (ii) saturation of the lowest-energy excitonic state A1, which leads to more $F1_{mod}$ emission from the $A1_{mod}$ state, or perturbation of one of the Chls contributing to the A1 state (i.e., with its site energy shifted blue) what in turn leads to higher energy lowest excitonic state and blue-shifted emission.

4.5. Comment on ZPH-Action Spectra. With regard to previously published ZPH action spectra,[17] one should note that the low-energy absorption tail in CP47 extends up to ~703 nm (see Figure 1), while the highest burning wavelength to generate the ZPH-action spectrum used in ref 17 was only ~692 nm. This made the proper assignment of the red-shifted A1 trap with a maximum at ~693 nm difficult. It has been shown in Figure 8 that the fluorescence spectrum from ref 17 (frame B) was contributed to by F1, FT1, and FT2 emissions. Hence, the broad Gaussian profile with a maximum at ~688.9 ± 0.4 nm and a width of ~200 cm^{-1} obtained in ref 17 should be in part contributed by SDF_{A1}, SDF_{AT1}, and SDF_{AT2} bands with the major contribution from the SDF_{AT1} near 690 nm. In reference to data shown in section 3.6, we conclude that in the CP47 samples all shallow holes required to generate ZPH-action spectrum should be obtained on fresh (i.e., unburned) samples to avoid problems associated with possible saturation of the lowest-energy state and possible secondary burning phenomena.

4.6. On the Contribution Originating from the Chls Absorbing at ~684 nm (AT2 Band). A well resolved shoulder near 683 nm is clearly observed in the absorption spectrum of Figure 1A. This absorption is most likely associated with the red state near 684 nm (AT2 band) as revealed by transient hole at 683.8 nm (see inset of Figure 6A) and FT2 emission near 685 nm. The ~684 nm state has been previously observed in singlet−triplet (T-S)[22] and transient HB spectra.[20] It is germane to notice the absence of a transient hole in sample 1B. We do not think that the presence of a transient hole indicates that EET times from at least some of these pigments are low enough to be competitive with intersystem crossing to the triplet state for these species, as suggested in ref 38; rather, we suggest that the transient hole is only observed in destabilized complexes for which the 684 nm state (AT2 band) is the lowest-energy state.

Previously, an oscillator strength for the ~684 nm state of about three Chls and excitonic character were assigned to this state.[38] In the same reference[38] an oscillator strength of ~1 Chl was assigned to the ~690 nm band (in our nomenclature band AT1; see Table 1); it was argued that the large red-shift is due to hydrogen (H) bonding to a protein ligand, although this assignment was later dropped based on new pump−probe data;[40] the feasibility of this assignment is further discussed in ref 27. At this point we can only speculate on the possible origin of

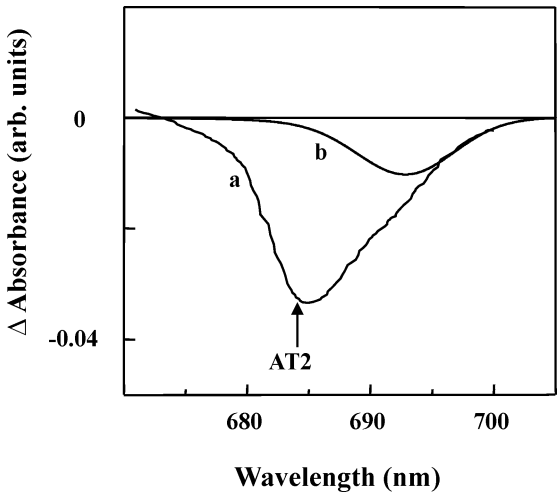

Figure 11. Curve a corresponds to the SADS spectrum of CP47 adopted from Figure 7 in ref 19, which was obtained on a few ns time scale. Curve b (expanded to fit the lowest-energy tail of spectrum a) is the A1 band from Figure 7B (this work). The upward arrow below curve (a) indicate possible contribution to the SADS spectrum from the AT2 trap.

the ~684 nm (AT2) band. As argued above, we believe that it is the lowest-energy trap in fractions of strongly destabilized CP47 complexes. Thus, we conclude that the EET in intact CP47 complexes occurs on a ps time-scale, and the emitting AT2 state reflects behavior of non-native complexes.

4.7. Comparison of HB Results with Literature Pump−Probe Data. EET in isolated CP47 complexes has also been studied by time-resolved absorbance-difference and fluorescence spectroscopies.[19] The absorption spectrum from the latter paper was very similar to that shown in Figure 1A. Thus it is of interest to compare the results of 77 K pump−probe analysis (where the pump and probe beams were set at the magic angle as reported in ref 19) with the data reported in this manuscript. We do not attempt to discuss the SADS connecting various lifetimes resulting from the global fit,[19] but based on the results reported above, it is very likely that the CP47 sample under consideration contained substantial fractions of destabilized complexes with FT1 and FT2 emissions, in addition to the F1 emission (~695 nm) originating from intact (undisturbed) complexes (a contribution from the $F1_{mod}$ emission due to high fluences used in these experiments also cannot be excluded). If this were the case, it is nearly impossible to interpret the excited-state dynamics in terms of bands obtained from the deconvolution of these "mixed" steady-state absorption spectra. Thus we will comment only on the SADS spectra obtained on the long time scale. Figure 11 shows such a spectrum that was obtained on a few ns time scale (see curve a adopted from Figure 7 of ref 19). Similar data were observed for a time-scale of 500 ps; see ref 19. Curve (a) in Figure 11 demonstrates that on this time scale (comparable to the fluorescence lifetime of CP47 complexes[17]) all energy is in the respective lowest energy state(s), presumably states A1 near 693 nm (see downward arrow), and a mixture of lowest-energy AT2 traps of destabilized complexes at 683.8 nm and the $A1_{mod}$ state (whose contribution is fluence dependent). Curve b in Figure 11 is the inverted A1 band from Figure 7. Spectrum b was expanded to fit the lowest-energy tail of spectrum a. The solid arrow indicates a contribution from AT2.

Thus we believe that the EET in both major fractions of CP47 complexes, i.e., complexes with the lowest energy trap AT1 near 689 nm (sample 1A) and trap A1 (near 693 nm (sample 1B), is fast as revealed by the width of the resonant holes burned near 680 nm in both samples. That is, as discussed above the total dephasing time at 680 nm was similar in both the 1A and 1B samples. (To get the EET time value, we have also assumed that spectral diffusion at 4.5 K is negligible). Thus, we concur with the major conclusion of ref 19 that EET for excitation near 680 nm is fast in both intact and destabilized CP47 samples, and as a result it should not contribute to the suggested slow trapping of excitation energy model in PSII.[38,41−43]

5. Conclusions

We have shown that absorption, emission, and persistent NPHB spectra of CP47 complexes, diluted from solutions stored at high optical density followed by sonication, dark thermal equilibration, and mixing with cryoprotectants (50/50 *v*/*v*) shortly before experimentation, exhibit less contribution from destabilized complexes and provide new insight into the nature of the electronic structure of intact CP47. The present work establishes that the lowest-energy state of CP47 is near 693 nm, i.e., energetically below the primary electron-donor state of the PSII RC that is expected to lie near 685 nm.[44−46] This means that at room temperature the energy of the primary electron-donor state is within reach of thermal energy *kT*. The lowest Q_y-state (~693 nm, A1 band) is characterized by weak electron−phonon coupling with a Huang−Rhys factor $S \sim 1 \pm 0.2$ and an Γ_{inh} of 180 cm^{-1}. The mean phonon frequency of the lowest energy trap A1 is 20 cm^{-1}. HB and absorption data indicate that the A1 state has a small oscillator strength; that is, it is much smaller than the oscillator strength corresponding to one Chl, in contrast to earlier assignments.[19,38] This in turn suggests that Chls absorbing at higher energies steal a significant amount of the oscillator strength from Chls contributing to the A1 trap, in agreement with a positive antihole feature at high energy in the persistent nonresonant hole spectra (see Figure 2). This fact should help to identify the A1 state pigments (see excitonic calculations in ref 27). Fluorescence of intact complexes was shown to be strongly dependent on the excitation power density. Different maxima of fluorescence spectra reported in the literature are attributed to varying contributions from several distinct emission bands (F1, FT1, and FT2) originating from intact and destabilized CP47 complexes, as well as potentially from shifts in these fluorescence bands due to HB if high-fluence was used. The above conclusions are consistent with the ZPH-action spectra obtained in absorption mode, the profiles of the nonresonantly and resonantly burned holes, as well as the FLN spectra obtained for the Q_y band. Importantly, intact CP47 complexes do not reveal any contribution from triplet-bottleneck (transient) holes, which were previ-

(40) Groot, M.-L.; Breton, J.; van Wildern Luuk, J. G. W.; Dekker, J.; van Grondelle, R. *J. Phys. Chem.* **2004**, *108*, 8001–8006.
(41) Miloslavina, Y.; Szczepaniak, M.; Müller, M. G.; Sander, J.; Nowaczyk, M.; Rögner, M.; Holzwarth, A. R. *Biochemistry* **2006**, *45*, 2436–2442.
(42) Schatz, G. H.; Brock, H.; Holzwarth, A. R. *Biophys. J.* **1988**, *54*, 397–405.
(43) Andrizhiyevskaya, E. G.; Frolov, D.; van Grondelle, R.; Dekker, J. P. *Phys. Chem. Chem. Phys.* **2004**, *6*, 4810–4819.
(44) Hughes, J. L.; Krausz, E.; Smith, P. J.; Pace, R. J.; Riesen, H. *Photosynth. Res.* **2005**, *84*, 93–98.
(45) Jankowiak, R.; Rätsep, M.; Hayes, J.; Zazubovich, V.; Picorel, R.; Seibert, M.; Small, G. J. *J. Phys. Chem. B* **2003**, *107*, 2068–2074.
(46) Jankowiak, R.; Tang, D.; Small, G. J.; Seibert, M. *J. Phys. Chem.* **1989**, *93*, 1649–1654.

ously observed in singlet-minus-triplet spectra, suggesting that the transient hole near 684 nm originates from partially destabilized complexes. Finally, we suggest that the absorption spectrum of intact CP47 reported in this work along with the absorption spectrum of the CP43 complex published recently[13] should allow extraction the real absorption spectrum of the intact reaction center residing in the intact PSII core complexes and shed more light on possible contaminations, charge-transfer emission in PSII core from spinach, and unusual fluorescence temperature dependence observed previously in CP47 complexes.

Acknowledgment. This work was performed at K-State and was supported by a U.S. Department of Energy (US-DOE) EPSCoR grant (R.J.) (DE-FG02-08ER46504) and the supplements from the Office of Basic Energy Sciences (US-DOE) and the Kansas Technology Enterprise Corporation. Partial support was also provided by the Office of Science, US-DOE (M.S.; NREL Contract DE-AC36-08GO28308), and the PN I+D+I of Spain (R.P.; AGL2008-00377). V.Z. acknowledges support by NSERC Discovery Grant.

JA908510W